

Relay Hindsight Experience Replay: Self-Guided Continual Reinforcement Learning for Sequential Object Manipulation Tasks with Sparse Rewards

Yongle Luo^{1,2}, Yuxin Wang^{1,2}, Kun Dong^{1,2}, Qiang Zhang¹, Erkang cheng¹, *Member, IEEE*, Zhiyong Sun¹, *Member, IEEE*, and Bo Song^{#1}, *Member, IEEE*

Abstract—Exploration with sparse rewards remains a challenging research problem in reinforcement learning (RL). Especially for sequential object manipulation tasks, the RL agent always receives negative rewards until completing all sub-tasks, which results in low exploration efficiency. To solve these tasks efficiently, we propose a novel self-guided continual RL framework, Relay-HER (RHER). RHER first decomposes a sequential task into new sub-tasks with increasing complexity and ensures that the simplest sub-task can be learned quickly by utilizing Hindsight Experience Replay (HER). Secondly, we design a multi-goal & multi-task network to learn these sub-tasks simultaneously. Finally, we propose a Self-Guided Exploration Strategy (SGES). With SGES, the learned sub-task policy will guide the agent to the states that are helpful to learn more complex sub-task with HER. By this self-guided exploration and relay policy learning, RHER can solve these sequential tasks efficiently stage by stage. The experimental results show that RHER significantly outperforms vanilla-HER in sample-efficiency on five single-object and five complex multi-object manipulation tasks (e.g., Push, Insert, ObstaclePush, Stack, TStack, etc.). The proposed RHER has also been applied to learn a contact-rich push task on a physical robot from scratch, and the success rate reached 10/10 with only 250 episodes.

Index Terms—Deep reinforcement learning, Robotic manipulation, Continual Learning, Residual Policy Learning

I. INTRODUCTION

Deep reinforcement learning (RL) has made many breakthroughs in various sequential decision-making problems, ranging from playing Atari [1], Go [2] to control tasks [3], especially for a number of robotic manipulation tasks such as grasping [4], door opening [5] and object manipulation [6].

However, it is still challenging to learn policies for sequential object manipulation tasks with sparse rewards. Due to receiving negative reward signals (e.g., $r = -1$) until completing tasks, the agent can not distinguish which action is better according to these identical negative rewards. Few valuable samples contribute to guiding policy optimization [7], which results in exponential sample complexity [8].

With HER [6], the agent can generate non-negative rewards (e.g., $r = 0$) by goal relabeling strategy to alleviate the negative sparse reward problem, even if the agent did not complete the

task. For simple reach tasks, the agent can benefit from HER in efficiency.

But for complex sequential object manipulation tasks, the agent still suffers from low sample efficiency with HER, due to another implicit sparse reward problem. For these sequential manipulation tasks, the agent needs to accomplish each sub-task before it can achieve the final desired goal. As shown in Fig. 1, in a toy push task, the agent needs to reach the object and push it to a desired position. But if the agent is unable to change the object position, the achieved goals (i.e., the object position) are identical in the whole episode. Thus, the hindsight goals are also identical, which means that all hindsight rewards are non-negative. The agent can not distinguish which action is better from these original samples or hindsight samples. We call this phenomenon as non-negative sparse reward (NNSR) problem. In general, when the agent’s ability is not enough to change the outcome of complex tasks, it still uses HER to change the goals to fantasize about success. This kind of ambitious behavior will not only be unhelpful for policy improvement, but even reduce the exploration ability of network [9] due to a large number of valueless non-negative hindsight samples.

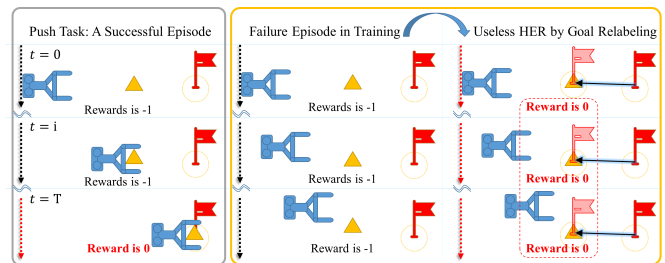


Fig. 1. Illustration of the problem of non-negative sparse rewards with HER. For a typical sequential task, push task, the agent fails to push the object to the desired position, and even fails to change the object position. So all original rewards are -1, and all hindsight rewards are 0, the latter can also be regarded as a kind of sparse reward problem, but with non-negative rewards.

To solve these complex sequential tasks with sparse rewards more effectively, the agent needs to affect the corresponding achieved goals, which will alleviate the above implicit NNSR problem by HER. So we propose a novel self-guided continual RL framework, Relay-HER (RHER). Firstly, RHER decomposes the whole sequential task into multiple stages (or steps) and then combines them to new sub-tasks with increasing complexity. Secondly, inspired by one-hot encoding, a multi-goal & multi-task network can be designed by a goal space

This work is supported in part by the grant of KRDP of Anhui Province (201904a05020086), NSFC(61804100, 61973294, 61806181) and CAS (GJTD-2018-15).

¹Institute of Intelligent Machines, Hefei Institutes of Physical Science, Chinese Academy of Sciences, Hefei, 230031, China

²University of Science and Technology of China, Hefei 230026, China

[#]Corresponding author, email: songbo@iim.ac.cn

The project is available at <http://github.com/kaixindelele/RHER>

encoding technique. With this structure, the agent can learn multiple sub-tasks with different complexity goals simultaneously. Third, the agent generates valuable non-negative samples for the accessible stages by using HER. Finally, a Self-Guided Exploration Strategy (SGES) is proposed. With SGES, the agent will be guided by the learned simpler policy to states that can change the achieved goal of a more complex sub-task with high probability. In other words, the agent can extend the accessible stages quickly by SGES. More efficient exploration is realized via self-guidance without human demonstrations or pre-defined controllers. The complex sequential tasks can be solved efficiently by this relay policy learning stage by stage.

The contributions of this study can be summarized as follows:

(1) For common complex sequential manipulation tasks with sparse rewards, this paper develops an elegant and sample-efficient self-guided continual RL framework, RHER.

(2) To achieve self-guided exploration, we propose a multi-goal & multi-task network to learn multiple sub-tasks with different complexity simultaneously.

(3) The proposed RHER method is more sample-efficient than vanilla-HER and state-of-the-art methods, which are validated in the standard manipulation tasks from the OpenAI Gym [10];

(4) To verify that the RHER is suitable for common sequential object manipulation tasks, we conduct three extra typical single-object tasks, five more complex multi-object tasks, and even a physical robot task.

II. RELATED WORK

Many studies try to deal with complex sequential object manipulation tasks under sparse rewards for more efficiency.

A. HER-based methods

HER paves a promising path toward the sparse reward problem. Through the Universal Value Function Approximators (UVFA) [11] with neural networks, it can even be generalized to the unseen actual goal. HER has extremely high efficiency in handling long-horizon reaching tasks [6], [12], but it is not efficient in sequential manipulation tasks.

In order to improve the sample efficiency of HER, many variants of HER have been proposed: **1)** curriculum learning to maximize the diversity of achieved goals [8], [13]; **2)** providing demonstrations [14], **3)** generating more valuable desired goals [15]; **4)** curiosity-driven exploration [16]; **5)** model-based RL methods [17]. These methods have improved the performance of HER to a certain degree, but none of these methods directly solve the NNSR problem.

The problem of identical achieved goals of HER is firstly reported in [18], the solution of which is to directly filter those ‘biased’ transitions with $r(s_{t-1}, a_{t-1}, g') = 0$. This method improves the sample efficiency compared to the vanilla-HER for three throwing tasks. However, it is not suitable for the common manipulation tasks when the goal space is within the workspace because these transitions can “teach” the agent not to destroy the achieved goal. The problem is further discussed in [8]. The researchers propose a SHER algorithm that learns

a reaching policy first and then transfers the reaching policy to a more complex sub-task. However, SHER can not learn multiple sub-tasks simultaneously, so it has no self-guided exploration.

B. Hierarchical RL with HER

To simplify the sequential manipulation tasks, many works combine hierarchical RL (HRL) with HER to solve these sub-tasks [19], [20]. Specifically, [20] effectively solves the stacking problem of three blocks in different orders by abstract demonstrations, *block-gripper-informed goals* and auto-adjusting exploration strategy. However, these HRL methods do not explicitly use the learned policy to guide a more complex policy during exploration, so the efficiency has not been improved enough. In addition, the *block-gripper-informed goals* is not suitable for some tasks, in which the target position of the gripper can not be set in advance, such as pushing tasks.

C. Continual learning and Continual-RL

Different from the aforementioned HER-based or HRL-based algorithms, this study adopts the continual RL scheme to solve sequential robotic tasks. CL has drawn increasing attention from the RL community over the last few years.

Current mainstream CL has three solutions to keep the previous tasks from forgetting [21]. The first is the regularization-based scheme [22], [23]. The second is the modular approaches [24], [25], for example, by designing a task-conditioned architecture, it can accommodate both previous and new tasks [21]. The third is the memory-based method which needs to revisit previous task data when training for a new task [26], [27]. The proposed RHER use a novel task-condition architecture and an inherent experience buffer of RL to avoid forgetting.

For object manipulation tasks, few methods use Deep RL with CL. [28] trains a hyper-network to get dynamics models with different dynamics tasks. To sidestep the exploration dilemma, this work places the object close to the gripper. [29] filters out samples not suitable for the target task, then relabel the remaining samples to pre-train a separate policy for a new task. In addition, both articles use a heuristic reward function.

In contrast to the above continual RL methods, RHER can share data across all sub-tasks by goal relabeling, nor do we need to design a heuristic reward function for each task, which means that it can be adapted to various tasks and scenarios with little effort.

III. PRELIMINARIES

This section introduces the background of RHER, including goal-conditioned RL and HER.

A. Goal-conditioned RL

According to the HER methods, manipulation tasks can be modeled as a finite-horizon, discounted Markov Decision Process (MDP). For a goal-conditional RL, the whole state S contains not only the observation S_o , but also a desired

goal S_{dg} , where $S_{dg} \in \mathcal{S}_o$. The policy $\pi_\theta(a_t | s_{o_t}, s_{dg_t})$ is usually a neural network model that maps the t step state $s_t = (s_{o_t}, s_{dg_t})$ to the action $a_t \in \mathcal{A}$. The MDP has some other necessary components: a discount factor $\gamma \in (0, 1)$, horizon length T and a reward function $r: \mathcal{S} \times \mathcal{A} \rightarrow \mathcal{R}$. The goal of the agent is to acquire an optimal policy $\pi_\theta(a | s_o, s_{dg})$ that maximizes the expected sum of discount rewards.

It is noted that any off-policy actor-critic algorithms or variants of HER can be used in the proposed RHER. As for the classic DDPG [30] algorithm, there are two main parts, an actor neural network denoted as $\pi_\theta(a | s_o, s_{dg})$, for generating actions, and a critic network denoted as $Q_\phi(s_o, s_{dg}, a)$, for evaluating the action performance. To stabilize the learning process, there is also a set of target actor π'_θ and target critic Q'_ϕ with the same structure but delayed update. The critic network parameter ϕ is learned by minimizing the Bellman error, and the loss function is defined as (1),

$$Loss_\phi^{(j)} = |Q_\phi(s_{o_t}, s_{dg_t}, a_t) - y_t|^2, \quad (1)$$

where the target $y_t = r_t + \gamma Q'_\phi(s_{o_{t+1}}, s_{dg_{t+1}}, a_{t+1})$; a_{t+1} is generated by $\pi'_\theta(s_{o_{t+1}}, s_{dg_{t+1}})$. To extend multi-task setting, let $s_{dg_t}^{(j)}$ denote the desired goal of j^{th} task.

Based on the Q function, the policy network parameter θ is trained using the gradient descent method with the loss represented as (2),

$$Loss_\theta^{(j)} = -\mathbb{E}_{s_{o_t}, s_{dg_t}^{(j)}} Q[s_{o_t}, s_{dg_t}^{(j)}, \pi_\theta(s_{o_t}, s_{dg_t}^{(j)})]. \quad (2)$$

Usually, the reward feedback is sparse, represented as (3),

$$r(s_{o_{t+1}}, s_{dg_{t+1}}, a_t) = -\mathbb{I}(s_{ag_{t+1}} = s_{dg_t}), \quad (3)$$

where $\mathbb{I}()$ is the indicator function, and $s_{ag_{t+1}} \in \mathcal{S}_{o_{t+1}}$ is the achieved goal in the next state. This reward function indicates whether the current task was completed.

B. HER Goal Relabeling

To use HER, we specify the following concepts:

- **desired goal**: the goal of the current episode, specifically, which is usually a target position.
- **achieved goal**: the goal achieved in the current state. It represents the end-effector position in a reaching task, whereas the object position in a manipulation task.
- **hindsight goal**: in experience replay, the HER method uses the future achieved goal in the episode as a hindsight goal.

According to vanilla-HER, with a probability of 0.8, we relabel the original desired goal s_{dg_t} with another observation from a future time step of the same episode as (4):

$$s_{dg_t}^h = s_{ag_{t+k}}, 1 \leq k \leq T, \quad (4)$$

where the $s_{dg_t}^h$ is the hindsight goal for t time step, $s_{ag_{t+k}}$ is the achieved goal for $t+k$ time step, and T is the last time step of the episode.

IV. METHODS

This section presents a novel self-guided continual RL framework, RHER. Four key components of RHER cooperate with each other to realize self-guided exploration, which enables the agent to quickly solve the complex sequential object manipulation tasks, as shown in Fig. 2.

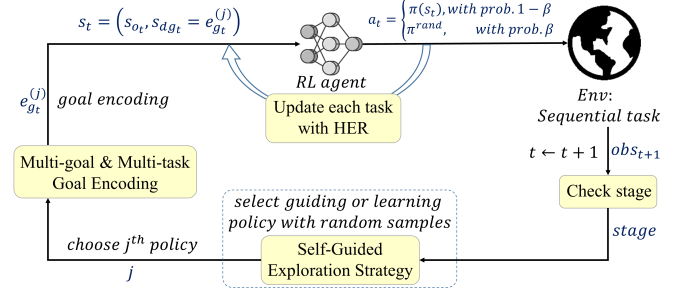


Fig. 2. A diagram of RHER, of which the key components are shown in the yellow rectangles. This framework achieves self-guided exploration for a sequential task.

According to the logical order of design, the four components are: **1)** The first component is to decompose the original sequential task into M stages (or steps) and then combine them to M sub-tasks with increasing complexity; **2)** The second component is to design a multi-goal & multi-task RL model to deal with the above sub-tasks simultaneously; **3)** By utilizing HER, this component overcomes the problem of negative sparse rewards and shares data collected from different sub-tasks; **4)** To collect more valuable samples and alleviate the NNSR by HER for sequential tasks, a Self-Guided Exploration Strategy (SGES) is proposed. The SGES uses a learned policy to guide the agent quickly to more complex stages. Through this self-guided exploration, agents can learn sequential tasks stage by stage, similar to a relay.

As a continual RL framework, the combination of these components realizes a stable knowledge transfer from a simple policy to a complex one and ensures that the simple policy will not be forgotten.

The full RHER algorithm is described in Algorithm 1 and the details of these four parts are introduced as follows.

Algorithm 1: Relay Hindsight Experience Replay

```

Initialize the agent and replay buffer R
for each episode do
  Sample an observation dictionary
  for each time step do
    Check stage as (6)
    Sample an action with SGES as (10)
    Execute the action and get new observation
    Store the transition
  for each gradient step do
    for each sub-task do
      Sample a mini-batch episodes  $B$  from R
      Replace the goal  $e_g^{(j)}$  as (9)
      Perform optimization of (1), (2) based on  $B$ 

```

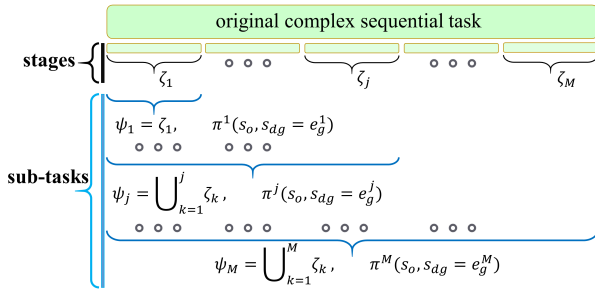


Fig. 3. Sequential task decomposition and rearrangement.

A. Task Decomposition and Rearrangement

In this paper, we decompose the original sequential task into M crucial stages ($\{\zeta_j | j = 1, 2, \dots, M\}$) and rearrange them to M new sub-tasks ($\{\psi_j | j = 1, 2, \dots, M\}$) with increasing complexity. As shown in Fig. 3, ψ_j is given by

$$\psi_j = \cup_{k=1}^j \zeta_k, \quad j \in \{1, 2, \dots, M\}, \quad (5)$$

The corresponding policy of ψ_j is denoted as π^j . Note that if the current stage is ζ_j , which means that the agent has solved the stages from ζ_1 to ζ_{j-1} . In addition, the policy π^j can handle the stages from ζ_1 to ζ_j , and π^1 just can deal with the ζ_1 .

If there are N objects to manipulate in order, this sequential task can be divided into $2N$ stages (i.e., $M = 2N$), according to the natural order of task. To be specific, the aim of $(2i-1)^{th}$ stage $\zeta_{(2i-1)}$ is to reach the i^{th} object and prepare for the $(2i)^{th}$ stage, and the $(2i)^{th}$ stage $\zeta_{(2i)}$ is to manipulate the i^{th} object to reach its target goal.

The distance from the end-effector to object d needs to be defined in advance (ablation experiments are shown in Section VI-C). The current stage index j can be determined by (6),

$$j = \begin{cases} 2 * i - 1 & \text{if } dist_i > d \\ 2 * i & \text{if } dist_i \leq d \end{cases} \quad (6)$$

where $dist_i$ is the distance between the end-effector and the i^{th} object. If $N > 1$, it means that the first $(i-1)^{th}$ objects have been solved.

According to (5), we rearrange the above stages into $M = 2N$ new sub-tasks. Considering that some manipulations, such as pushing and sliding, require continuous decision-making, this task rearrangement is necessary. A detailed ablation study will be conducted to discuss the relationship between the sub-tasks and stages (see Section VI-B).

For a more concrete example, in a two-block pushing task, the 2^{nd} stage ζ_2 is that the end-effector has reached the 1^{st} object, but neither of the blocks has reached the specified location; the 3^{th} stage ζ_3 represents that the 1^{st} object has been moved to its target, but the second one hasn't, and the end-effector is far from the second ones. The 3^{th} sub-task ψ_3 means that: 1) reach the 1^{st} block, 2) push the 1^{st} block to the desired location, 3) leave the 1^{st} block and keep it in position, then reach the position of 2^{nd} block.

B. Multi-goal & Multi-task RL Model

When the original complex task is decomposed into $2N$ new tasks with increasing complexity, an intuitive solution is to use the idea of CL to resolve these sub-tasks in order. The objective of CL is to learn new knowledge of the current task continuously, while the performance on previous tasks is not forgotten. In this manner, a network structure that can deal with multiple sub-tasks is required. The standard multi-task RL policy can be denoted as (7):

$$\pi_{\theta}(a | s_o, s_{dg}^{(j)} = e_g^{(j)}), \quad (7)$$

where $a \in A$ represents the action comprised of a 4-D vector for controlling 3-D position and 1-D opening of the gripper in this study; $s_o \in S$ represents the system states comprised of Cartesian positions, the linear velocity of the gripper and the position and velocity information of the object; $s_{dg}^{(j)}$ represents the desired goal of ψ_j ; $e_g^{(j)}$ represents the specific goal space encoding of $s_{dg}^{(j)}$.

Task-ID	goal encoding	Goal space: s_{dg}			Sub-task Description
		g^{grip}	g^{obj^1}	g^{obj^2} g^{obj^3}	
1	$e_g^1 = (ag^1, \mathbf{0}^3, ag^2, ag^3)$	ag^1	$\mathbf{0}^3$	ag^2, ag^3	Reach obj^1
2	$e_g^2 = (\mathbf{0}^3, dg^1, ag^2, ag^3)$	$\mathbf{0}^3$	dg^1	ag^2, ag^3	Push obj^1
3	$e_g^3 = (ag^2, dg^1, \mathbf{0}^3, ag^3)$	ag^2	dg^1	$\mathbf{0}^3, ag^3$	Push obj^1 & Reach obj^2
4	$e_g^4 = (\mathbf{0}^3, dg^1, dg^2, ag^3)$	$\mathbf{0}^3$	dg^1	dg^2, ag^3	Push obj^1 & Push obj^2
5	$e_g^5 = (ag^3, dg^1, dg^2, \mathbf{0}^3)$	ag^3	dg^1	$dg^2, \mathbf{0}^3$	Push obj^1 & Push obj^2 & Reach obj^3
6	$e_g^6 = (\mathbf{0}^3, dg^1, dg^2, dg^3)$	$\mathbf{0}^3$	dg^1	dg^2, dg^3	Push obj^1 & Push obj^2 & Push obj^3

Fig. 4. An example of multi-goal & multi-task goal space encoding for a three-object push task. ag^i is the achieved goal of obj^i (i.e., the current position of obj^i); dg^i is the desired goal of obj^i ; $\mathbf{0}^3$ is 3-D zero vector which plays a key role in the task identity.

Designing an elegant and effective $e_g^{(j)}$ is a key prerequisite for the following self-guided exploration. The traditional multi-task network depends on a one-hot task ID with the state as inputs [4], [24]. However, one-hot goal representations are not suitable for continuous goal space.

To design a multi-goal & multi-task network, inspired by the one-hot encoding, we use the zero-padding encoding (i.e., a 3-D zero vector $\mathbf{0}^3$) to identify tasks.

We take a complex three-object task as an example, as shown in Fig. 4. In this sequential task, three objects are denoted by obj^i ($i = 1, 2, 3$), the corresponding position of these objects are denoted by ag^i ($i = 1, 2, 3$), and the corresponding goal are denoted by dg^i ($i = 1, 2, 3$). To perform the task, six sub-tasks, i.e. $\{\psi_j | j = 1, 2, \dots, 6\}$ are defined through (5). The goal space s_{dg}^j consists of g^{grip} , g^{obj^1} , g^{obj^2} and g^{obj^3} , which are the goals of gripper and three object respectively. The aim of ψ_1 is to reach obj^1 , so the goal of the gripper, i.e. g^{grip} is the current position of the obj^1 , i.e. ag^1 . Noted that, because the agent can not affect the obj^1 in this stage, the goal of obj^1 , g^{obj^1} , is replaced by $\mathbf{0}^3$, which also can distinguish the present task from others. In addition, g^{obj^2} and g^{obj^3} are ag^2 and ag^3 , respectively, which mean that ψ_1 should not change the current position of these objects. Another typical sub-task is ψ_4 , the aim of ψ_4 is to push obj^1 and obj^2 to original desired goal

dg^1 and dg^2 respectively. Thus, the g^{grip} is replaced with $\mathbf{0}^3$, g^{obj^1} is dg^1 , g^{obj^2} is dg^2 , the g^{obj^3} is also ag^3 to keep obj^3 in position.

Obviously, according to the above encoding rule, $e_g^{(j)}$ depends on the number of objects, i.e. N and specific task index, i.e. (j) . What's more, the encoding of two-object is a simpler version of three-object, and the single-object is also a simpler version of two-object. For brevity, we only give the typical formulation here, for $N > 6$, $6 < j < 2N - 4$, and $i = (j + 1) \lfloor 2$, the $e_g^{(j)}$ can be formulated as (8):

$$e_g^{(j)} = \begin{cases} [ag^i || dg^1 \dots dg^{i-1} || \mathbf{0}^3 || ag^{i+1} \dots ag^N], & \text{if } j = 2i - 1, \\ [\mathbf{0}^3 || dg^1 \dots dg^{i-1} || dg^i || ag^{i+1} \dots ag^N], & \text{if } j = 2i, \end{cases} \quad (8)$$

Such a multi-goal & multi-task encoding serves as the foundation of the following data transfer and self-guided exploration.

C. Maximize the Use of All Data by HER

When a network that can handle these multi-goal & multi-task is developed, it will generate plenty of data during the process of exploration, not only from failure experiences but also from different policies.

The CL methods aim to transfer knowledge effectively. In the RHER framework, updating a policy can not only use its own explored data but also relabel the data collected by other policies by HER.

Coincidentally, for continual RL, the agent also needs to generate non-negative samples by HER. Specifically, to update the policy $\pi^{(j)}$ of ψ_j , a transition $(s_t, a_t, s'_t, s_{dg} = e_{g_t})$ will be sampled from a trajectory jointly explored by different policies. Then the original goal encoding e_{g_t} will be replaced by $e_{g_t}^{(j)}$ as (8) with probability 0.2, and the hindsight goal as (9) with probability 0.8:

$$e_{s'_t}^{(j)} = \begin{cases} [gp_{t+k}^i || ag_{t+k}^1 \dots ag_{t+k}^{i-1} || \mathbf{0}^3 || ag_{t+k}^{i+1} \dots ag_{t+k}^N], & \text{if } j = 2i - 1, \\ [\mathbf{0}^3 || ag_{t+k}^1 \dots ag_{t+k}^{i-1} || ag_{t+k}^i || ag_{t+k}^{i+1} \dots ag_{t+k}^N], & \text{if } j = 2i, \end{cases} \quad (9)$$

where gp_{t+k}^i is the $t+k$ time step gripper position, $t < k < T$, and the T is the trajectory length, which follows the *future* strategy from [6].

Therefore, the RHER scheme can realize both the forward and backward data transfer together for CL, and alleviate the negative sparse reward problem by HER.

D. Self-Guided Exploration Strategy (SGES)

Compared with standard CL, continual RL not only needs to share data but also needs to actively interact with the environment to obtain new valuable data, and even needs online exploration to eliminate the accumulation of errors of inference caused by offline data.

What's more, as mentioned in Section (I), due to the NNSR problem, the agent needs to collect more useful samples, which denotes that the corresponding achieved goals need to

be changed by the agent. Therefore, an efficient and stable exploration strategy is required.

Inspired by the idea of a relay, when a traveler needs to explore further, he/she needs to be escorted by some experts, then he/she can quickly pass through the area that the expert is familiar with, and finally explore new areas by himself/herself. Also like students for scientific research, who are guided by advisers and other researchers until they need to explore a new field.

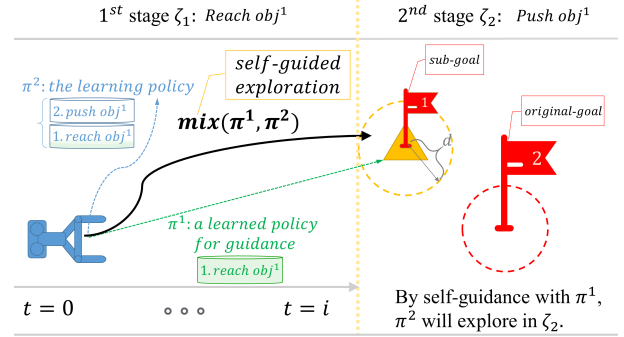


Fig. 5. Illustration of Self-Guided Exploration Strategy (SGES) in a toy push task.

As for robotic manipulation tasks, the RL agent can be guided by itself with RHER. The agent learns the simplest sub-task quickly by HER because the corresponding achieved goals can be changed by the agent all the time. We use this learned policy as a guide-policy, and the next more complex one as a learning-policy. RHER mixes the learning-policy and guide-policy in the sub-task that the latter has learned. Even though the learning-policy deviates a little from the optimal trajectory at first, the guide-policy can correct it in time. Thus, the agent can quickly reach the next stage to collect new valuable data for the learning-policy.

An example diagram can be found in Fig. 5. The learned reach policy π^1 can directly reach the object in ζ_1 , and the trajectory of a learning policy π^2 is far away from the object. When π^1 and π^2 are mixed in ζ_1 , the trajectory is corrected to reach the object. Therefore, the agent can quickly collect valuable samples for π^2 by this self-guidance.

The closest related work is the Residual-RL, which expects to combine the strengths of a model-based controller and Deep RL in two different ways. The first way is to superpose the signals of both policies [31], [32]. What these studies have in common is that the guide-policies are fixed and contain prior knowledge. The second way is to select a policy according to the certain probability [33], [34], which is suitable for this work because the guide-policy will be updated online. In this manner, we mix policies with the same probability in SGES. To the best of our knowledge, we present the first method to realize self-guidance exploration without any pre-defined controller.

Such a self-guidance exploration strategy introduces the second hyper-parameter, i.e., the probability α of the guide-policy. A detailed ablation study will be conducted to show that this hyper-parameter is also insensitive (see Section VI-D). Specifically, for exploration in RHER, the current stage index

j can be checked by (6) and the action is selected according to (10):

$$a = \begin{cases} \pi^r & \text{with/prob. } \beta, \\ \pi^{\max(g,j)} & \text{with/prob. } \alpha, \\ \pi^{\min[\max(g,j)+1,2N]} & \text{with/prob. } 1 - \alpha - \beta, \end{cases} \quad (10)$$

where π^r is a random policy, the probability of random actions is β , α is the guide probability, and g is the guide stage index which means the corresponding test success rate of π^g beyond a pre-defined threshold sr . In this work, for simple single-object tasks, $sr = 1.0$, for complex multi-object tasks, $sr = 0.8$.

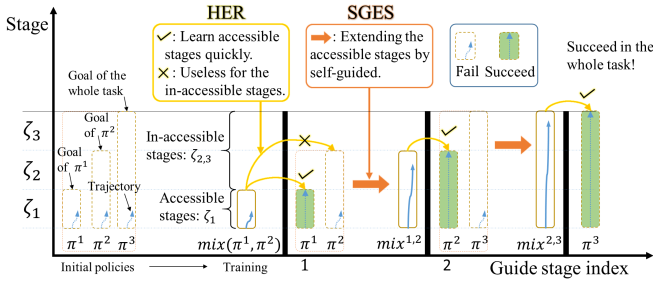


Fig. 6. A diagram of relay policy learning for a task with 3 stages. By using HER and SGES, RHER can solve the whole sequential task stage by stage with sample efficient.

By the four components of RHER, the RL agent can solve the original complex sequential tasks with sparse rewards efficiently stage by stage. In short, by using HER, the agent can learn the accessible stages quickly, while by using SGES, the agent can extend the accessible stages quickly with self-guidance. A detailed relay policy learning diagram can be seen in Fig. 6.

V. EXPERIMENTAL SETUP

In this section, the setup of six single-object, five multi-object simulations, and a real robot experiment are introduced to answer the following questions:

- How does RHER compare with vanilla-HER in terms of efficiency and final performance?
- How sensitive is RHER to the two new hyper-parameter?
- How well does RHER perform in preventing forgetting and transferring knowledge across tasks?
- Does RHER scale to more complex multi-objects tasks and a real-world scenario?

A. Setup of the Simulation Environments

Three standard simulations are conducted in the gym fetch manipulation environments: FetchPush, FetchPickAndPlace, and FetchSlide. To illustrate that RHER can be generalized to other manipulation tasks, three additional single-object tasks are carried out. To illustrate that RHER can solve complex manipulation tasks, five multi-object tasks are conducted. These new tasks are shown in Fig. 7. The details are elaborated as follows.

Drawer : 1) Reach the handler, and 2) slide the drawer to a target position by pulling the handler.

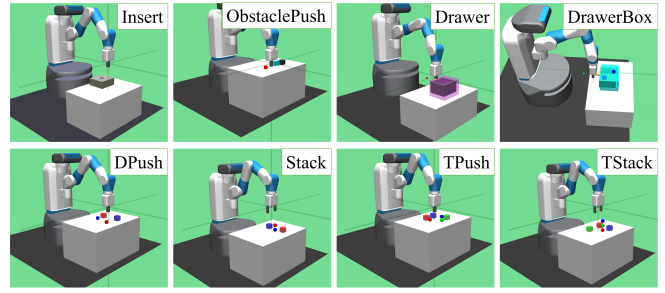


Fig. 7. Different sequential object manipulation tasks. The single-object tasks are Insert, ObstaclePush and Drawer. The two-object tasks are DrawerBox, DPush and Stack. The three-object tasks are TPush and TStack.

Insert : 1) Reach the hole, 2) insert a closed gripper into a hole with a random position. This paper creatively sets a virtual object in the inserting task, when the gripper reaches the vicinity of the hole, the virtual object will be moved by the gripper, so that HER can be applied.

ObstaclePush : 1) Reach the block, 2) push the block to a desired position in the presence of an obstacle that is unknown in size and shape.

DPush : 1) Reach the first block, 2) push the first block to a desired position, 3) leave the first block and reach the second, and 4) push the second block to another desired goal.

Stack : 1) Reach the first block, 2) grasp the first block to a desired position, 3) leave the first block and reach the second, 4) grasp the second block on the top of the first block.

DrawerBox : 1) Reach the handler, 2) slide the drawer to a target position by pulling the handler, 3) reach the block, 4) grasp the block on the top of the drawer.

TPush : There are three blocks to push in order.

TStack : There are three blocks to stack in order.

The reward functions are still the most common binary rewards described in (3). The other settings are referred to [6] (details can be found in **Gym**).

B. Setup on a Physical Robot

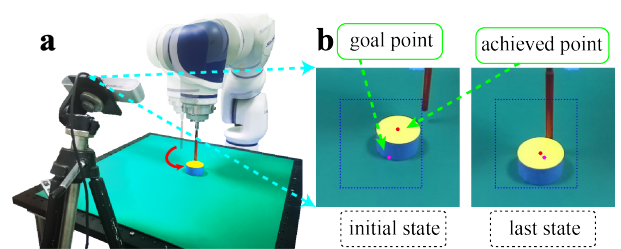


Fig. 8. CuePush: the real-world testing rig consists of a 7-DoF robot arm and a target cylinder. (a) A color-based camera detection system measures the Cartesian positions of the cylinder. (b) For the initial state, it samples a random point as the desired goal from the valid range.

CuePush : 1) reach a wooden cylinder, 2) push it to a desired position.

As shown in Fig 8, the cylinder is 2.5 cm in radius and 3 cm in height, the end-effector is a metal cue that is attached at the end of a 7-DOF manipulator (SCR5, Siasun. Co, Shenyang, China), with the positions of the cue and the cylinder extracted by a monocular camera (ZED, Stereolabs, San Francisco, CA,

US). This study even executes an open-loop automatic reset script to avoid human bias. Limited by the automatic reset script, the workspace of the robotic arm controlled by RL is only 9×14 cm. Therefore, the distance threshold d in the simulation is reduced from 5 cm to 2 cm.

C. Default Details of the Training Procedure

For each episode, the agent performs 40 optimization steps on mini-batches of size 256 sampled uniformly from a replay buffer consisting of $1e6$ transitions. The network structure and input scaling are default as [12].

Multi-processing training: Since the sample efficiency and the performance of the HER increases with the number of parallel training processes [12], the proposed method is compared to the baselines in a multi-processing setting to validate its superiority.

In this setting, 50 epochs are trained with 19 CPU cores (one epoch consists of $19 \times 50 = 950$ full episodes), in which each episode consists of 50 steps.

Single-processing training: Considering that there is usually only one robotic arm for online learning in the real world, we also make a comparison with vanilla-HER in a single-processing setting. Due to the lower sample diversity of single-processing, the vanilla-HER learns the tasks with 1200 epochs.

In this setting, the RHER and HER have 400 and 1200 epochs, a total of 400×50 and 1200×50 episodes, respectively, in which each episode consists of 50 steps. For the real environment, 15 epochs are set for training, and each episode just has 20 steps.

VI. RESULTS

This section demonstrates the efficiency and effectiveness of RHER compared with baselines (HER). Ablation experiments will be conducted to illustrate the effect of each component or hyper-parameter. Three extra single-object tasks are carried out to show the generality of the RHER. Five more complex multi-object manipulation tasks further illustrate the broad application potential of RHER. Finally, the real-world experiment shows that the model-free RL can also be learned from scratch in real with sparse rewards.

A. Comparison with Baselines

Multi-processing: As shown in Fig. 9b, RHER achieves dramatically higher sampling efficiency, better performance, and lower variance (less sensitive to random seeds) in FetchPush and FetchPickAndPlace. However, in the FetchSlide task, the performance of RHER is slightly worse than that of vanilla-HER. This may be due to the FetchSlide task being more sensitive [35], and the goal space is beyond the workspace, which is not suitable for RHER.

Single-processing: As shown in Fig. 9(d), in the single-processing cases, the HER exhibits quicker learning as well as more stable performance. To be specific, the method proposed needs only 78K interaction steps (31 epochs) to achieve a success rate of 95% in the FetchPush task, demonstrating sample efficiency 17 times higher than that of the vanilla-HER

(550 epochs). Counter-intuitively, it is shown that the single-processing cases have higher sample efficiency compared with the multi-processing because the latter wastes more sampling opportunities in the early stage. Therefore, the results show that RHER has more potential to be applied to realistic scenarios.

Continual RL: For continual RL, it is necessary to evaluate whether the previous tasks are forgotten as the training process proceeds. As shown in Fig. 9(a), (c), the policies of the previous task (ψ_1) can converge quickly without guidance whether in the multi-processing or the single-processing case, which proves that the previous tasks are retained by the multi-goal & multi-task encoding all the time.

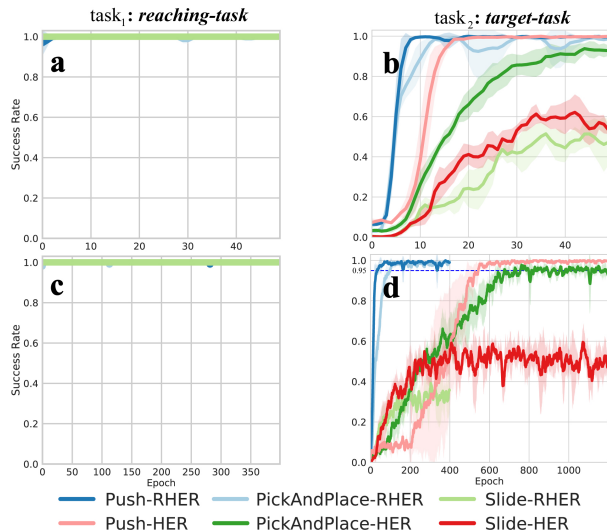


Fig. 9. Learning curves for the *reaching-tasks* and *target-tasks*. Results are shown over 5 independent runs. The training curve represents the mean with standard deviation (based on 5 independent runs). (a) The *reaching-tasks* learning curves with multi-processing training. (b) Learning curves of *target-tasks* for multi-processing training. (c) Learning curves of *reaching-tasks* for single-processing training. (d) Learning curves of *target-tasks* for single-processing training.

B. Ablation 1: Policy Combinations in ζ_1

Comparison among Combinations: First, according to the task decomposition (see Section IV-A), the original task is divided into $2(N=1)$ stages (ζ_1, ζ_2), but what kind of policy combination needs to be determined. As shown in Table I, for training or testing, ζ_1 can be processed by π^1 and π^2 so that there are three policy combinations: π^1 , π^2 , and a mix of π^1 and π^2 , denoted as (π^1, π^2) . When the ζ_1 is processed only by π^2 in training, it is the same as the original HER, thereby excluding this option. There remain $2 \times 3 = 6$ combinations and the corresponding results of these six cases are shown in Fig. 10. For example, for Case0, the agent mixes the π^1 and π^2 to explore the ζ_1 in training, whereas π^2 in testing (ζ_2 can only be solved by π^2). It can be seen from Fig. 10, that only Case0 (ours) takes into account both performance and efficiency.

Other Results: There are some other interesting results in Fig. 10. 1) In Case4, π^2 does not explore ζ_1 in the training process, so it cannot handle ζ_1 . This is largely attributed to the

distributional shifts of actor-critic models using offline data. Details can be found in Fig. 12, which shows that π^2 requires a certain percentage of exploration to correct bias from offline data. 2) Combined with Case1, Case2, and Case0, the results show that, in testing, the performance of π^2 is damaged by other policies. The visualization results for the push task show that π^1 usually pushes the object out of the threshold, so the agent also takes π^1 for the next time step until the object fell off the table. The counter-intuitive result is caused because two policies cannot be toggled well. These results also explain the necessity of our task rearrangement formulation as (5).

Through the above experiments, an appropriate policy combination (Case0) that satisfies both efficiency and performance can be determined.

Table I. Different combinations of policies in the previous stage (ζ_1).

Case	Case0(Ours)	Case1	Case2	Case3	Case4	Case5
Training	(π^1, π^2)	(π^1, π^2)	(π^1, π^2)	π^1	π^1	π^1
Testing	π^2	π^1	(π^1, π^2)	π^1	π^2	(π^1, π^2)

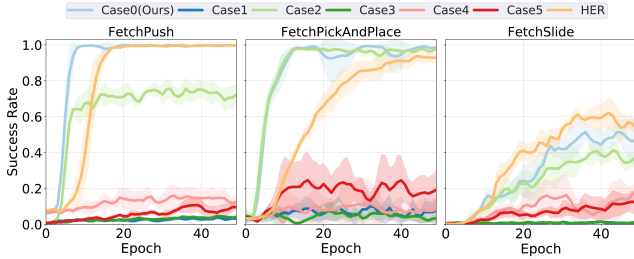


Fig. 10. Ablation study of task rearrangement. Details of these cases are described in Table I

C. Ablation 2: Distance Threshold

This subsection evaluates the effect of the distance threshold d on performance. This is the first hyper-parameter introduced by RHER, which will affect the efficiency of exploration. However, Fig. 11 shows that if d is too large ($d = 0.12m$), the performance will be degraded because the agent will also be hard to affect the achieved goals of the ψ_2 . If it is too small ($d = 0.0m$), it will hinder from learning the ψ_2 . However, as long as this distance is slightly larger ($d \in \{0.03m, 0.05m\}$) than the size of the object ($0.025m$), the performance is highly sample-efficient. In other words, this hyper-parameter can be easy to choose.

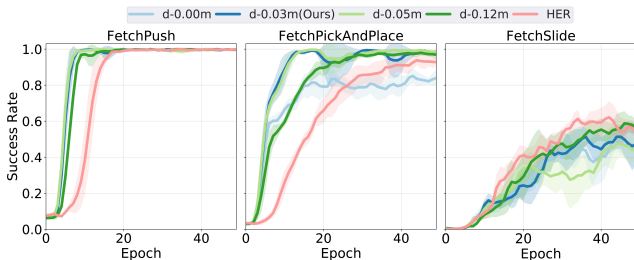


Fig. 11. Ablation study of different distance thresholds between gripper to the object.

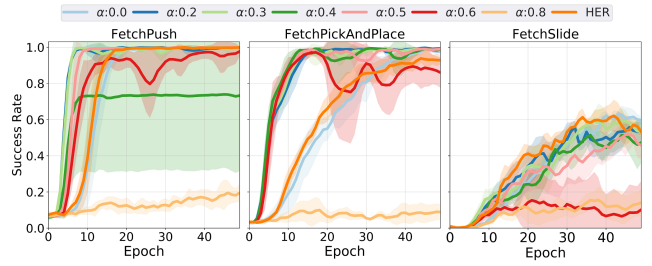


Fig. 12. Ablation study of exploration rate of SGES. Where the ratio of random policy π^r is fixed at 0.2, α is the sampling probability of the guide-policy π^1 in ζ_1 .

D. Ablation 3: The Rate of Guide-policy in SGES

This subsection evaluates the guidance rate in ζ_1 , which is the second hyper-parameter in RHER. As shown in Fig. 5, in the reaching stage, there are three policies, the reaching policy π^1 , the target policy π^2 , and the random policy π^r . In this study, we fix the probability of π^r as 0.2 and then increase the probability of the guidance policy π^1 . From Fig. 12 it is clear that as long as there is guidance ($\alpha \in \{0.2, 0.3, 0.4, 0.5, 0.6\}$) by π^1 , the target policy π^2 will be accelerated. It confirms that SGES is a crucial element that makes the exploration more effective.

Interestingly, for two extreme cases, the experimental results can dispel some doubts. If there is no guidance from π^1 in ζ_1 ($\alpha = 0.0$), the agent uses the offline data to train an auxiliary task, such as a ψ_1 , which does not speed up the ψ_2 . If there is no exploration of π^2 in ζ_1 ($\alpha = 0.8$), the agent is unable to solve the ψ_2 by using offline data from π^1 .

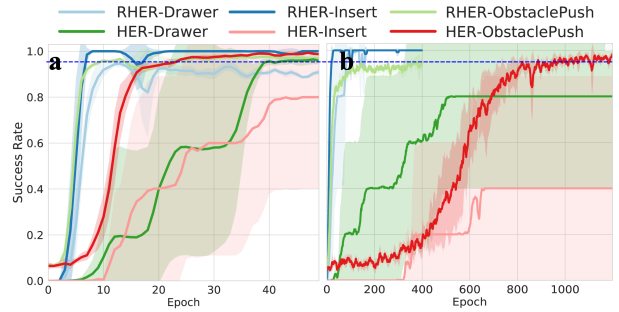


Fig. 13. Learning curves for three extended single-object tasks compared with vanilla-HER in (a) multi-processing and (b) single-processing.

E. Extending RHER to Three Extra single-object Tasks

To validate the robustness of RHER, three extended and typical single-object tasks are conducted with the same hyper-parameters as the above three classical tasks. As shown in Fig. 13, in three challenging tasks, RHER still maintains high exploration efficiency and good performance, especially in single-processing. It is noted that RHER learns the Insert task from scratch within 65K time steps, which may have a positive impact on the industry. In contrast, vanilla-HER has a very high variance in all tasks, which means that some random seeds can be lucky to explore valuable data, while others remain stuck in local optima.

F. Extending RHER to Five Multi-object Tasks

To verify the effectiveness of self-guided exploration and relay policy learning, the RHER algorithm need to be test on more complex multi-object manipulation tasks.

Compared with the single-object tasks, the complexity of the multi-object task increases significantly. For example, the three-object tasks need to be divided into six stages, and it is also necessary to consider the relative position of other objects while moving one object. Therefore, we update the previous implement: 1) We used a PyTorch implementation of the TD3 [36] method instead of the above the Tensorflow of DDPG. 2) To allow the agent to quickly learn the latest sub-task, we changed the st mentioned in (10) from 1.0 to 0.8, which means that we select the most complex learned sub-task policy as the guide-policy. 3) Due to the samples with more diversity, the mini-batch size needs to be increased from 256 to 2048. 4) To stabilize the learned stages, we adapt the AAES methods from [20]. 5) Finally, due to the difficulty of the multi-object tasks, we increased the episode length of two-object and three-object from 50 to 60 and 70 respectively.

After making the above modifications, we tested it on three two-object tasks as shown in Fig. 7. One novel task is the DrawerBox, which is a common challenging kitchen manipulation task. In addition, there are more complex three-object manipulation tasks.

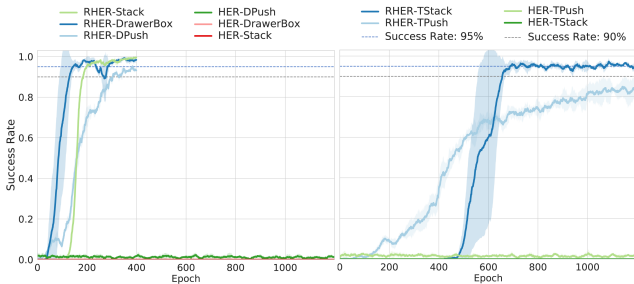


Fig. 14. The curves of test success rate of multi-object tasks. The left and right parts show the results of two-object tasks and three-object tasks, respectively.

As shown in Fig. 14, the RHER can still learn these complex sequential tasks quickly, while vanilla-HER can not learn even the simplest two-object tasks. Specifically, for two-object tasks, the success rate of RHER reaches 90% less than $300 \times 50 = 15K$ episodes, while the ACDER [16] needs more than $150 \times 500 = 75K$ episodes (as reported in their paper). As for TStack, RHER reaches an average success rate of 95% after roughly $700 \times 50 = 50K$ episodes. But for the TPush task, the final performance rises slower, because this task requires more complex trajectory compared to TStack.

In summary, by self-guided exploration and relay policy learning, RHER can address complex sequential object manipulation tasks efficiently with sparse rewards without any human demonstrations or pre-defined model controllers.

G. Learning on A Physical Robot from Scratch

In CuePush, the end-effector is a smooth cue, and the object is a cylinder. As a result, the task is hard to design a suitable controller, and the automatic reset script usually

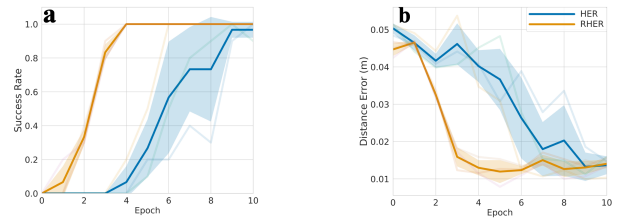


Fig. 15. The curves of test success rate and distance error on CuePush.

pushes the object off the reset goal so that it needs to take multiple attempts. However, RHER learns this push task with the success rate of 10/10 within 5K steps (250 episodes) and reduces the distance error to about 1cm, which is still efficient and stable, as shown in Fig. 15. If the workspace is larger, there will be more improvement compared with vanilla-HER.

H. Comparison with State-of-the-art Methods

To further evaluate the sample efficiency of RHER, a comparison of RHER with other HER-based state-of-the-art algorithms in the literature can be found in Table II. Since some papers do not release their code, this study uses the results of their paper for comparison. We compare the number of interactions required when achieving the same mean test success rate of 95%. Even though the IHER is a type of model-based method and ACDER has dynamic initial states to alleviate the non-negative sparse rewards, RHER still requires minimal interactions in two standard robotic tasks, as shown in Table II.

Table II. Number of interactions needed for test success rate 95% in Push and Pick task with SOTA methods.

	FetchPush(95%)	FetchPickAndPlace(95%)
vanilla-HER [16]	580K	1680K
ACDER [16]	110K	260K
IHER [17]	~80K	~300K
RHER(ours)	78K	250K

VII. DISCUSSION AND CONCLUSION

In this paper, we propose a concise self-guided continual RL framework, called RHER, which solves complex sequential object tasks extremely efficiently with sparse rewards. The simulation experiments show that RHER can achieve stable and efficient performance on five single-object and five multi-object manipulation tasks, especially in the single-processing training. Finally, we trained an agent to complete the push task from scratch on a physical robot, requiring only 5K interaction steps. These results indicate that RHER is generalized to object manipulation tasks and that RHER has application potential for real tasks without building a corresponding simulation. It is worth mentioning that this relay-style idea can inspire multi-agent or hierarchical RL, and the self-guided idea can be extended to other tasks (e.g., using a policy trained with a sub-optimal dense reward function to guide a policy with a sparse reward function, etc.). In future work, we will extend our approach to other RL domains.

REFERENCES

- [1] V. Mnih, K. Kavukcuoglu, D. Silver, A. A. Rusu, J. Veness, M. G. Bellemare, A. Graves, M. Riedmiller, A. K. Fidjeland, G. Ostrovski *et al.*, “Human-level control through deep reinforcement learning,” *nature*, vol. 518, no. 7540, pp. 529–533, 2015.
- [2] D. Silver, A. Huang, C. J. Maddison, A. Guez, L. Sifre, G. Van Den Driessche, J. Schrittwieser, I. Antonoglou, V. Panneershelvam, M. Lanctot *et al.*, “Mastering the game of go with deep neural networks and tree search,” *nature*, vol. 529, no. 7587, pp. 484–489, 2016.
- [3] J. Schulman, F. Wolski, P. Dhariwal, A. Radford, and O. Klimov, “Proximal policy optimization algorithms,” *arXiv preprint arXiv:1707.06347*, 2017.
- [4] D. Kalashnikov *et al.*, “Mt-opt: Continuous multi-task robotic reinforcement learning at scale,” *arXiv:2104.08212*, 2021.
- [5] S. Gu, E. Holly, T. Lillicrap, and S. Levine, “Deep reinforcement learning for robotic manipulation with asynchronous off-policy updates,” in *2017 IEEE international conference on robotics and automation (ICRA)*. IEEE, 2017, pp. 3389–3396.
- [6] M. Andrychowicz *et al.*, “Hindsight experience replay,” in *Advances in Neural Information Processing Systems*, 2017, pp. 5048–5058.
- [7] K. Hartikainen *et al.*, “Dynamical distance learning for unsupervised and semi-supervised skill discovery,” *arXiv:1907.08225*, 2019.
- [8] B. Manela *et al.*, “Curriculum learning with hindsight experience replay for sequential object manipulation tasks,” *Neural Networks*, vol. 145, pp. 260–270, 2022.
- [9] H. Sun, L. Han *et al.*, “Exploiting reward shifting in value-based deep rl,” *arXiv preprint arXiv:2209.07288*, 2022.
- [10] G. Brockman *et al.*, “Openai gym,” *arXiv:1606.01540*, 2016.
- [11] T. Schaul *et al.*, “Universal value function approximators,” in *International conference on machine learning*. PMLR, 2015, pp. 1312–1320.
- [12] M. Plappert *et al.*, “Multi-goal reinforcement learning: Challenging robotics environments and request for research,” *arXiv:1802.09464*, 2018.
- [13] M. Fang *et al.*, “Curriculum-guided hindsight experience replay,” *Advances in Neural Information Processing Systems*, vol. 32, 2019.
- [14] A. Nair *et al.*, “Overcoming exploration in reinforcement learning with demonstrations,” in *2018 IEEE international conference on robotics and automation*. IEEE, 2018, pp. 6292–6299.
- [15] P. Liu *et al.*, “Generating attentive goals for prioritized hindsight reinforcement learning,” *Knowledge-Based Systems*, vol. 203, p. 106140, 2020.
- [16] B. Li *et al.*, “Acder: Augmented curiosity-driven experience replay,” in *2020 IEEE International Conference on Robotics and Automation*. IEEE, 2020, pp. 4218–4224.
- [17] R. McCarthy *et al.*, “Imaginary hindsight experience replay: Curious model-based learning for sparse reward tasks,” *arXiv:2110.02414*, 2021.
- [18] B. Manela *et al.*, “Bias-reduced hindsight experience replay with virtual goal prioritization,” *Neurocomputing*, vol. 451, pp. 305–315, 2021.
- [19] A. Levy, G. Konidaris, R. Platt, and K. Saenko, “Learning multi-level hierarchies with hindsight,” *arXiv preprint arXiv:1712.00948*, 2017.
- [20] X. Yang *et al.*, “Hierarchical reinforcement learning with universal policies for multistep robotic manipulation,” *IEEE Transactions on Neural Networks and Learning Systems*, 2021.
- [21] J. von Oswald *et al.*, “Continual learning with hypernetworks,” in *International Conference on Learning Representations*, 2019.
- [22] A. Benjamin *et al.*, “Measuring and regularizing networks in function space,” in *International Conference on Learning Representations*, 2018.
- [23] R. Aljundi, F. Babiloni *et al.*, “Memory aware synapses: Learning what (not) to forget,” in *Proceedings of the European Conference on Computer Vision*, 2018, pp. 139–154.
- [24] C. Rosenbaum *et al.*, “Routing networks: Adaptive selection of non-linear functions for multi-task learning,” in *International Conference on Learning Representations*, 2018.
- [25] F. Alet *et al.*, “Modular meta-learning,” in *Conference on Robot Learning*. PMLR, 2018, pp. 856–868.
- [26] A. Chaudhry *et al.*, “Efficient lifelong learning with a-gem,” in *International Conference on Learning Representations*, 2018.
- [27] M. Riemer *et al.*, “Learning to learn without forgetting by maximizing transfer and minimizing interference,” in *International Conference on Learning Representations*, 2018.
- [28] Y. Huang *et al.*, “Continual model-based reinforcement learning with hypernetworks,” in *2021 IEEE International Conference on Robotics and Automation*. IEEE, 2021, pp. 799–805.
- [29] A. Xie and C. Finn, “Lifelong robotic reinforcement learning by retaining experiences,” *arXiv:2109.09180*, 2021.
- [30] T. P. Lillicrap *et al.*, “Continuous control with deep reinforcement learning,” *arXiv preprint arXiv:1509.02971*, 2015.
- [31] G. Schoettler *et al.*, “Deep reinforcement learning for industrial insertion tasks with visual inputs and natural rewards,” in *2020 IEEE/RSJ International Conference on Intelligent Robots and Systems*. IEEE, 2020, pp. 5548–5555.
- [32] R. Zhang *et al.*, “Residual policy learning facilitates efficient model-free autonomous racing,” *IEEE Robotics and Automation Letters*, pp. 1–8, 2022.
- [33] F. Fernández and M. Veloso, “Probabilistic policy reuse in a reinforcement learning agent,” in *Proceedings of the fifth international joint conference on Autonomous agents and multiagent systems*, 2006, pp. 720–727.
- [34] T. Silver *et al.*, “Residual policy learning,” *arXiv:1812.06298*, 2018.
- [35] X. Yang, Z. Ji *et al.*, “An open-source multi-goal reinforcement learning environment for robotic manipulation with pybullet,” in *Annual Conference Towards Autonomous Robotic Systems*. Springer, 2021, pp. 14–24.
- [36] S. Fujimoto, H. Hoof, and D. Meger, “Addressing function approximation error in actor-critic methods,” in *International conference on machine learning*. PMLR, 2018, pp. 1587–1596.